Wood Material Science & Engineering
Publication details, including instructions for authors and subscription information:
http://www.tandfonline.com/loi/swoo20

Ultraviolet resistance and other physical properties of softwood polymer nanocomposites reinforced with ZnO nanoparticles and nanoclay

Ankita Hazarika[a] & Tarun K. Maji[a]
[a] Department of Chemical Sciences, Tezpur University, Assam, India
Published online: 30 Jan 2015.

Wood Material Science & Engineering, 2015
http://dx.doi.org/10.1080/17480272.2014.992471

Taylor & Francis
Taylor & Francis Group

ORIGINAL ARTICLE

Ultraviolet resistance and other physical properties of softwood polymer nanocomposites reinforced with ZnO nanoparticles and nanoclay

ANKITA HAZARIKA & TARUN K. MAJI

Department of Chemical Sciences, Tezpur University, Assam, India

Abstract
Wood polymer nanocomposites (WPNCs) based on nano-ZnO and nanoclay were prepared by impregnation of melamine formaldehyde–furfuryl alcohol copolymer, 1,3-dimethylol-4,5-dihydroxyethyleneurea (DMDHEU), a cross-linking agent and a renewable polymer obtained as a gum from the plant *Moringa oleifera* under vacuum condition. Fourier transform infrared spectroscopy (FTIR) and X-ray diffractometry (XRD) studies were employed for the characterization of modified ZnO and WPNCs. The change in crystallinity index (CrI) value of the cellulose in wood and the distribution of ZnO nanoparticles in composites were determined using FTIR and XRD. Scanning electron microscopy and Transmission electron microscopy showed the presence of nanoparticles and nanoclay in the cell lumen or cell wall of wood. An enhanced UV resistance property was shown by the treated wood samples as judged by lower weight loss, carbonyl index, lignin index, cellulose CrI values, and mechanical property loss compared to the untreated wood samples. Wood polymer composites treated with 3 phr each of nanoclay, ZnO, and the plant gum showed an improvement in mechanical properties, flame-retarding properties, thermal stability, and lower water uptake capacity.

Keywords: *Composite materials, wood, polymers, thermal properties, mechanical properties*

Introduction

During the past few years, considerable interest has been developed in the field of nanocomposites due to their unique characteristics. The properties of a nanocomposite are significantly determined by the size of its constituent and the extent of mixing between the two phases (i.e., the polymers and nanofillers). In general, nanomaterials offer reinforcing capability due to their high aspect ratios. Nanocomposites possess many advantages over macrocomposites or conventional composites that include reduced filler amount and better properties such as high thermal stability, high mechanical strength, high chemical resistance, low gas permeability, good transparency, light weight, etc. Nanotechnology provides a striking method to prepare wood polymer composites (WPCs) using layered silicate clay, metal oxide nanofillers, carbon nanotubes, etc. Nanoclay-modified WPCs could produce valuable products with enhanced physical, thermal, and mechanical properties (Cai *et al.* 2008). Besides using clay, the incorporation of inorganic nanoparticles can afford further improvement in various properties like weather resistance, flame resistance, UV resistance, etc., which are very important properties of the WPCs (Devi and Maji 2012). The WPCs are used in diverse applications, from commercial buildings to industrial products. The products can be used for joints and beams that substitute steel in many building projects. The most common use of WPCs is in outdoor deck floors, but it is also used for park benches, fences, landscaping timbers, railings, molding and trim, cladding and siding, window and door frames, and indoor furniture. It is a cheaper alternative to plastic, wooden, and other sheets.

UV resistance is one of the most desirable properties of WPCs for outdoor applications. The shielding of UV irradiation is provided by the nanolayers of clay in polymer nanocomposite, but ZnO is a promising contender for an efficient UV absorber (Deka and Maji 2012). The surface of the ZnO was modified in order to enhance interaction with the wood and polymer (Hong *et al.* 2009).

Correspondence: T. K. Maji, Department of Chemical Sciences, Tezpur University, Assam 784028, India. Tel: 91 03712 267007 (Extn: 5053). Fax: 91 03712 267005. E-mail: tkm@tezu.ernet.in

(*Received 6 July 2014; revised 21 October 2014; accepted 24 November 2014*)

Furfuryl alcohol (FA) derived from biowaste such as sugar cane bagasse, corn cobs, etc., is reported to increase dimensional stability, weight percent gain (WPG), hardness, and durability of wood, but above all it is environment friendly (Venas and Rinnan 2008). It polymerizes in situ and permanently swells the cell walls (Schneider 1995, Lande *et al.* 2004). FA-treated wood does not have significant influence on the bending strength and the modulus of elasticity (MOE) (Esteves *et al.* 2011). Melamine formaldehyde resin can impart high thermostability, flame retardancy, mechanical properties, and high resistance to water attack and is capable of forming hydrogen bonds leading to an increase of the number of valuable properties of wood (Gindl *et al.* 2003, Bajia *et al.* 2009). A copolymer of melamine formaldehyde–furfuryl alcohol (MFFA) can be used as an impregnating material into wood in order to achieve an overall improvement in properties of the composites.

Wood is combustible in nature, and there is unremitting attempt to improve the fire-resistant properties of wood. Most of the fire retardants can easily leach to the surface and on burning produce harmful fumes and gases, which are highly perilous to the environment as well as to human health. The use of polymeric flame retardant can reduce the leaching problem and enhance the service life of the product (Devi *et al.* 2007). But these are not biodegradable and cause a serious threat to the environment. Polymeric flame retardant obtained from renewable resources, i.e., from a local plant *Moringa oleifera* will be ecofriendly, cheaper, and can minimize the leaching problem. Very few literatures are available on the use of this gum as a flame retardant (Ghosh and Maiti 1998, Jana *et al.* 2000).

Most of the available reports are based on wood polymer clay nanocomposites. However far less is available that relates the effect of renewable plant polymer and nano-ZnO to the wood polymer clay nanocomposites. A comprehensive study may provide some valuable information regarding formation of WPC.

In this study, wood polymer nanocomposites (WPNCs) have been prepared by impregnation of the MFFA copolymer, 1,3-dimethylol-4,5-dihydroxyethyleneurea (DMDHEU), a cross-linking agent, plant polymer collected as a gum from a local plant *Moringa oleifera* as a flame retarding (FR) agent, nanoclay, and ZnO. This work is focused to study the effect of ZnO and plant polymer on the physical, mechanical, flame retardant, thermal, and UV resistance properties of wood composites.

Experimental Materials and Methods

Materials

Fig wood (*Ficus hispida*) and the gum from the plant *Moringa oleifera* were collected from a local forest. Melamine, FA, glyoxal, and formaldehyde were purchased from Merck (Mumbai, India). Maleic anhydride was obtained from G.S. Chemical Testing Lab. & Allied Industries (India). Nanomer (clay modified by 15–35 wt% octadecylamine and 0.5–5 wt% aminopropyltriethoxy silane; Aldrich, USA), ZnO nanopowder (<100 nm; Aldrich, Germany), and N-Cetyl-N,N,N-trimethyl ammonium bromide (CTAB; Central Drug House (P) Ltd., Delhi, India) were used as received. All other chemicals used were of analytical grade.

Modification of ZnO

Surface modification of ZnO is a common approach to prevent agglomeration of nanosized particles in the polymer matrix. The cationic surfactant CTAB was used to modify the surface of ZnO nanoparticles for the homogenous dispersion of ZnO in the polymer. About 10 g of ZnO was taken in a round-bottom flask fitted with spiral condenser containing 1:1 ethanol–water mixture and stirred at 80°C for 24 h (ratio of ZnO and ethanol–water mixture is 0.1:10). About 12 g of CTAB was taken in another beaker containing ethanol–water mixture and stirred at 80°C for 6 h (ratio of CTAB and ethanol–water mixture is 0.14:10). The ZnO mixture was added to it and finally stirred for another 24 h. The mixture was then filtered and washed with deionized water for several times. Finally, it was dried overnight in vacuum oven at 45°C, ground, and stored in a desiccator to avoid moisture absorption. Thus, the modified ZnO would contain the long organic chain cetyl group and the surface hydroxyl groups, which lead to an enhancement in the interaction between ZnO, polymers, wood, and clay.

Preparation of the MFFA copolymer

Melamine and formaldehyde were taken in a molar ratio of 1:3 and polymerized by bulk polymerization method at 80–85°C by maintaining pH at 8.5–9.0 with Na_2CO_3. FA (1 mole) was added to the aqueous solution of methylol melamine followed by the addition of maleic anhydride as catalyst and finally polymerized for another 45 min. The viscosity (at 30°C) of different batches of MFFA copolymer thus prepared was almost similar as judged by Ubbelohde viscometer. The formation of copolymer has been confirmed by nuclear magnetic resonance (NMR) study from our previous study (Hazarika and Maji 2013).

Dispersion of nanoclay and ZnO in MFFA copolymer

Nanoclay and ZnO were swelled in FA–water mixture for 24 h with mechanical stirring. FA–water mixture can swell the nanoclay and is a good solvent for the MFFA copolymer. The dispersed nanoclay and ZnO were then sonicated for 30 min. Now MFFA was slowly added to the dispersed nanoclay and ZnO under stirring condition. The ratios of nanoclay, ZnO, and FA–water mixture were 3:1:20, 3:2:20, and 3:3:20. This mixture was further sonicated for 15 min. To this mixture, plant polymer dissolved in dimethylformamide (DMF)-water was added, stirred, and kept ready for use.

Preparation of DMDHEU cross-linker

Urea was slowly added to an aqueous solution of glyoxal under nitrogen purge. The pH of the reaction mixture was adjusted to approximately 5.5. The reaction mixture was heated to 50°C and allowed to stir for 24 h. It was cooled to room temperature, neutralized, and evaporated to near dryness by rotary evaporator to yield crude 4,5-dihydroxyethylene urea (DHEU). A portion of this DHEU was added to an aqueous formaldehyde solution and the pH was adjusted to 8.2–8.5. The molar ratio of *n*(glyoxal), *n*(urea), *and n*(formaldehyde) was taken as 1:1.10:1.95 for the synthesis of DMDHEU. The reaction mixture was heated to approximately 50°C and allowed to stir for 24 h. The reaction mixture was then allowed to cool to room temperature, neutralized, and kept for subsequent use. The formation of DMDHEU has been characterized by NMR in our previous work (Hazarika and Maji 2014).

Preparation of WPCs

All the samples were oven dried at 105°C to constant weight before treatment and dimensions and weights were measured. The samples were then taken in an impregnation chamber. Loads were applied over each sample to prevent them from floatation during the addition of the impregnating mixture. Vacuum was applied for a specific time period for removing the air from the pores of the wood samples before the addition of prepolymeric mixture. Now, the MFFA copolymer with maleic anhydride; or MFFA copolymer with maleic anhydride and DMDHEU; or MFFA copolymer with maleic anhydride, DMDHEU, nanoclay and ZnO; or MFFA copolymer with maleic anhydride, DMDHEU, nanoclay, ZnO and plant polymer was introduced into the impregnation chamber through a dropping funnel to completely immerse the sample. The samples were kept in the impregnation chamber for 6 h after attaining atmospheric pressure. After that, samples were taken out of the chamber and excess chemicals were wiped from the surfaces of the prepared composites. The samples were then wrapped in aluminum foil and cured at 90° C for 24 h in an oven. This was followed by drying at 105°C for another 24 h. The cured samples were then Soxhlet extracted to remove homopolymers, if any, formed during impregnation. The dimensions were further measured by using slide caliper, and weights were taken.

Weight percent gain

WPG after polymer loading was calculated according to the formula:

$$\mathrm{WPG}\ (\%) = (\mathrm{W}_2 - \mathrm{W}_1)/\mathrm{W}_1 \times 100$$

where W_1 was oven dry weight of wood blocks before polymer treatment and W_2 was oven dry weight of blocks after polymer treatment.

Volume increase (%)

Percentage volume increase after impregnation of wood samples was calculated by the formula:

$$\%\ \text{Volume increase} = (\mathrm{V}_2 - \mathrm{V}_1)/\mathrm{V}_1 \times 100$$

where V_1 was the oven dry volume of the untreated wood and V_2 was oven dry volume of the treated wood.

Hardness

The hardness of the samples was measured by using a durometer (model RR12) according to ASTM D-2240 method and expressed as shore D hardness.

Fourier transform infrared spectroscopy study

The treated and untreated samples were grinded, and Fourier transform infrared spectroscopy (FTIR) spectra were recorded by using KBr pellet in a Nicolet (Madison, USA) FTIR Impact 410 spectrophotometer.

X-ray diffraction analysis

The crystallographic studies were done by X-ray diffractometry (XRD) analysis using Rigaku X-ray diffractometer (Miniflax, UK) and employing CuKα radiation (λ = 0.154 nm), at a scanning rate of 2° min^{-1} with an angle ranging from 2° to 60°. The crystallinity index (CrI) was determined from XRD analysis using the following formula

$$\mathrm{CrI} = \mathrm{A}_{\mathrm{cryst}}/\mathrm{A}_{\mathrm{total}} \times 100,$$

where A_{cryst} is the area of the peak for 002 plane and A_{total} is the total area of the peak below the whole region.

Morphology of nanocomposites

The presence of different elements in the plant polymer and the composites were studied by energy-dispersive X-ray elemental analysis (EDX). The morphologies of untreated and treated wood samples were studied by using (JEOL JSM-6390LV) scanning electron microscope (SEM) at an accelerated voltage of 5–10 kV. The fractured surface of the samples was used for the study. These were sputtered with platinum and deposited on brass holder.

Transmission electron microscopy (TEM) was performed to study the dispersion of silicate layers and presence of ZnO nanoparticles. An ultramicrotome fitted with a diamond knife was used for ultrathin sectioning (approximately 100 nm thick) of the transverse film surfaces. The samples were embedded with epoxy resin for the preparations of (ultra) thin as well as polished sections. The sections were stained with 1% (wt%) uranyl acetate for sufficient contrast. The sections were then mounted on grids and examined with a JEOL JEM-2100 TEM at an accelerating voltage of 80 kV.

UV resistance test

The degradation study of the WPC samples was done in UV chamber (Model: S.L.W., voltage: 230 V; Advanced Research Co., India) using a mercury arc lamp system that produces a collimated and highly uniform UV flux in the 200 to 400 nm range. The exposure period varied from 0 to 60 days. The weight loss was measured and is expressed as follows:

$$\%\ \text{Weight loss} = (W_t - W_0)/W_0 \times 100$$

where W_t is the specimen weight at time t and W_0 is the specimen weight before exposure. The UV degradation was studied by FTIR analysis. The intensity of the carbonyl (C=O) stretching peaks at 1715 cm^{-1} in cellulose of untreated wood was measured. The net peak heights were determined by subtracting the height of the baseline directly from the total peak height. The same baseline was taken for each peak before and after exposure to UV (Stark and Matuana 2004). The carbonyl index was calculated using the following equation:

$$\text{Carbonyl index} = I_{1715}/I_{2924}(100)$$

where I represents the intensity of the peak. The peak intensities were normalized by using -CH stretching peak of alkane at 2924 cm^{-1}. This peak was chosen as reference due to its least change during irradiation. The lignin index (LI) of the wood was calculated for all the untreated and treated wood samples. It is the ratio of the height of the lignin characteristic band at 1510 cm^{-1} to that of the band at 2924 cm^{-1}. The band corresponding to C-H stretching of cellulose appeared at 2924 cm^{-1}, which is very stable to oxidation and remains constant throughout the UV exposure.

$$LI = I_{1510}/I_{2924}(100)$$

The possibility of change in cellulose crystallinity due to UV irradiation is determined by CrI. It is defined as the ratio of the areas of the bands at 1437 and 2924 cm^{-1}:

$$CrI = A_{1437}/A_{2924}$$

Surface morphology of UV-degraded specimen was characterized by SEM.

Mechanical property

The flexural strength of the samples was measured by UTM-HOUNSEFIELD, England (model H100K-S) with a cross-head speed of 2 mm/min and by calculating the MOE and modulus of rupture (MOR) according to ASTM D-790 method.

MOR was calculated as follows:

$$MOR = 3WL/2bd^2$$

Statistical analysis

Data for tensile and flexural values were expressed as mean ± standard deviation. Results were statistically analyzed using one-way analysis of variance followed by Tukey's honest significant difference (HSD) test. Five samples of each category were tested.

Limiting oxygen index

Limiting oxygen index (LOI) test was performed by using flammability tester (S.C. Dey Co., Kolkata) according to ASTM D-2863 method. The sample was placed vertically in the sample holder of the LOI apparatus. The ratio of nitrogen and oxygen at which the sample continued to burn for at least 30 s was noted.

$$\text{Limiting oxygen index (LOI)} = \text{Volume of } O_2/\text{Volume of } (O_2 + N_2) \times 100$$

Thermal property

Thermal properties of WPCs were measured in a thermogravimetric analyzer (TGA-50, Shimadzu) at

a heating rate of 10°C min^{-1} up to 600°C under nitrogen atmosphere.

Water uptake test

Both untreated and treated wood samples were immersed in distilled water at room temperature (30°C), and weights were taken after 0.5, 2, 6, 24, 48, 96, 120, 144, and 168 h. It is expressed as:

$$\text{Water uptake } (\%) = (W_t - W_d)/W_d \times 100$$

where W_d is the oven dry weight and W_t is the weight after immersion in distilled water for a specified time period.

Results and discussion

Various parameters like vacuum, time of impregnation, monomer concentration, initiator concentration, amount of cross-linking agent, nanoclay, and plant polymer were varied to obtain optimum properties. The conditions at which maximum improvement of properties were obtained were 500 mm Hg vacuum, 6 h time of impregnation, 5:1 (MFFA:FA–water) prepolymer concentration, 1% (w/w) maleic anhydride, 3 ml DMDHEU, 3 phr nanoclay, 3% w/v plant polymer (Hazarika and Maji 2013, 2014).

Effect of variation of ZnO on polymer loading (WPG%), volume increase, and hardness

From Table I, it was observed that the hardness of the composites increased due to impregnation of MFFA copolymer into wood. A significant improvement in polymer loading (WPG%), volume increase, and hardness was noticed when ZnO was impregnated along with MFFA, DMDHEU, and nanoclay into the wood. The fill up of the void spaces, pits, and capillaries of the untreated wood by the MFFA copolymer would lead to an enhancement in the WPG and volume increase thereby improving its hardness value. The deposition of MFFA in the void spaces were further enhanced by the use of the cross-linking agent DMDHEU as it can cross-link with the wood cell wall as well as with the hydroxyl and methylol group of MFFA through its own hydroxyl groups (Xie *et al.* 2010). The impregnation of nanoparticles, i.e., nanoclay and ZnO along with the polymers into the empty spaces of wood further improved the properties of wood. The improvements in properties were also observed with an increase in percentage of ZnO. The addition of plant polymer again enhanced the properties. The plant polymer contains mainly L-arabinose, D-galactose, D-glucuronic acid, L-rhamnose, D-mannose, and D-xylose (Bhattacharya *et al.* 1982), which have abundant hydroxyl groups. These hydroxyl groups facilitated interaction between the hydroxyl groups of wood, polymer, and nanoparticles.

FTIR study

The FTIR analysis of (a) MFFA, (b) DMDHEU, (c) plant polymer, (d) nanoclay, (e) ZnO, (f) CTAB-modified ZnO is represented in Figure 1. MFFA copolymer (curve a) showed bands at 3404 cm^{-1} (-OH stretching), 1566 cm^{-1} and 1508 cm^{-1} (furan ring vibration), 1186 cm^{-1} (C-N stretching) and 813 cm^{-1} (out-of-plane trisubstitution of triazine ring) (Lori *et al.* 2011). The absorption bands exhibited by DMDHEU (curve b) at 3418, 1702, 1245, 1021 cm^{-1} were for -OH stretching, C=O stretching, -CHOH stretching, and -CH_2OH stretching, respectively (Jang *et al.* 1993). The plant polymer (curve c) showed bands at 3431 cm^{-1} (-OH stretching), 2925 cm^{-1}, 2858 cm^{-1} (-CH_2 asymmetric and symmetric stretching), 1619 cm^{-1} (-OH bending), 1441 cm^{-1} (C-H bending in lignin and carbohydrates, O-H in-plane bending of cellulose), and 1376 cm^{-1} (-CH bending in cellulose and hemicelluloses, C-H bond in -O(C=O)-CH_3 group). In the spectrum of nanoclay (curve d), peaks appeared at 3465, 2932 and 2859, 1621, and 1031–457 cm^{-1} were for -OH stretching, -CH stretching of modified hydrocarbon, -OH bending and oxide bands of metals like Si, Al, Mg, etc. The absorption peaks at

Table I. Effect of variation of CTAB-ZnO on weight% gain (WPG%), volume increase and hardness.

Sample particulars	Weight % gain (WPG %)	Volume increase %	Hardness (Shore *D*)
Untreated		-	46 (±1.07)
Samples treated with MFFA/FA–water/DMDHEU/ Nanoclay/CTAB-ZnO/plant polymer			
100/20/3/0/0/0	28.13 (±0.47)	2.12 (±0.82)	62 (±0.76)
100/20/3/3/1/0	43.53 (±0.63)	3.32 (±0.28)	75 (±1.06)
100/20/3/3/2/0	46.88 (±0.49)	3.54 (±0.38)	77 (±0.57)
100/20/3/3/3/0	49.86 (±0.81)	3.98 (±1.03)	78 (±0.43)
100/20/3/3/3/3	50.91 (±0.75)	4.01 (±0.93)	79 (±0.37)

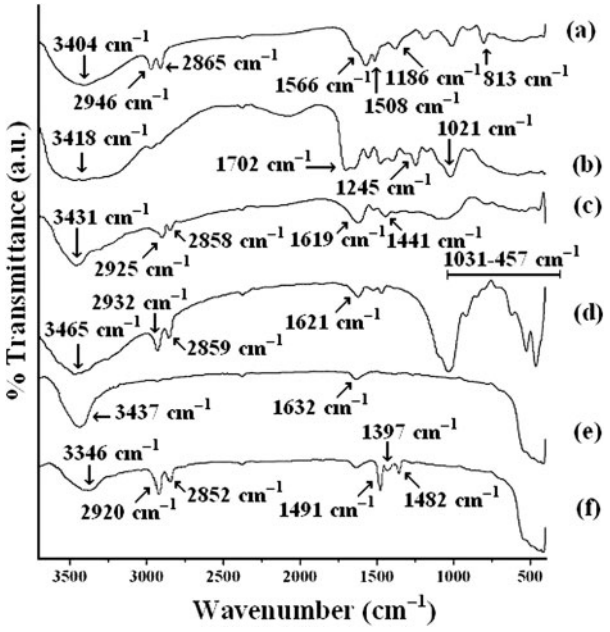

Figure 1. FTIR spectra of (a) MFFA, (b) DMDHEU, (c) plant polymer, (d) nanoclay, (e) ZnO, and (f) CTAB-modified ZnO.

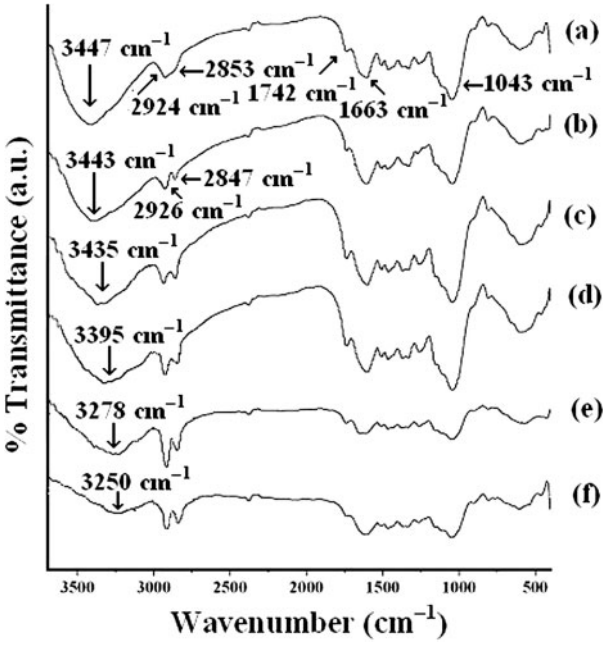

Figure 2. FTIR spectra of wood (a) untreated and treated with (b) MFFA/DMDHEU, (c) MFFA/DMDHEU/nanoclay/ZnO (1 phr), (d) MFFA/DMDHEU/nanoclay/ZnO (2 phr), (e) MFFA/DMDHEU/nanoclay/ZnO (3 phr), and (f) MFFA/DMDHEU/nanoclay/ZnO (3 phr)/plant polymer.

3437 and 1632 cm^{-1} in the spectrum of unmodified ZnO (curve e) could be assigned to -OH (-stretching) and -OH (-bending) vibrations and the peaks appeared at around 424 cm^{-1} was due to the vibration of metal–oxygen (M–O) bond. Curve f represents the FTIR spectrum of CTAB-modified ZnO. The intensity of the peak assigned for -OH group was decreased and shifted to wave number 3346 cm^{-1}. Moreover, two new peaks at 2920 and 2852 cm^{-1} due to the presence of $-CH_2$ group of CTAB appeared. Other notable peaks appeared at 1491 and 1482 cm^{-1} (asymmetric CH_3-N^+ deformation mode of the CTAB head group) and 1397 cm^{-1} (symmetric CH_3-N^+ deformation mode of CTAB head group) (Li and Tripp 2002). This indicated the incorporation of long chain of CTAB on the surface of the ZnO nanoparticles.

The FTIR analysis of wood (a) untreated and treated with (b) MFFA/DMDHEU, (c) MFFA/DMDHEU/nanoclay/ZnO (1 phr), (d) MFFA/DMDHEU/nanoclay/ZnO (2 phr), (e) MFFA/DMDHEU/nanoclay/ZnO (3 phr), and (f) MFFA/DMDHEU/nanoclay/ZnO (3 phr)/plant polymer is represented in Figure 2. Untreated wood (curve a) shows absorption bands at 3447 cm^{-1} (-OH stretching), 2924 cm^{-1}, 2853 cm^{-1} ($-CH_2$ asymmetric stretching in alkyl groups due to both cellulose and lignin), 1509 cm^{-1} (aromatic skeletal vibration by lignin), 1742 cm^{-1} (C=O stretching of hemicelluloses), 1663 cm^{-1} (-OH bending), 1258 and 1043 cm^{-1} (C–O stretching), and 1000–646 cm^{-1} (out-of-plane C–H bending vibration). In the curves b–f, it was observed that intensity of the peak corresponding to -OH stretching was decreased and shifted to 3443 cm^{-1} (curve b), 3435 cm^{-1} (curve c), 3395 cm^{-1} (curve d), and 3278 cm^{-1} (curve e). The decrease in intensity of hydroxyl group and shifting of the peak to lower wave number might be attributed to the participation of hydroxyl groups of clay and ZnO in the cross-linking reaction between wood, MFFA, and DMDHEU. Dhoke *et al.* (2009) studied the interaction between nano-ZnO particles and alkyd resin by FTIR analysis and found similar decrease in the intensity of hydroxyl group of alkyd resin. In the spectrum of plant polymer–treated wood/MFFA/DMDHEU/nanoclay/ZnO composite (curve f), the intensity of the -OH stretching peak was found to decrease further and shifted to lower wave number (3250 cm^{-1}). This further confirmed the participation of plant polymer in the cross-linking reaction. Moreover, in all the cases, the intensity of the peak for the -CH stretching at 2924 cm^{-1} was found to increase compared to that of peak of untreated wood. Similar observation on increase in peak intensity was reported by Deka and Maji (2010) while studying the FTIR analysis of WPCs treated with clay and ZnO.

XRD analysis

The XRD pattern of (a) unmodified ZnO, (b) CTAB-modified ZnO nanoparticles, (c) nanoclay is represented in Figure 3. All the characteristic

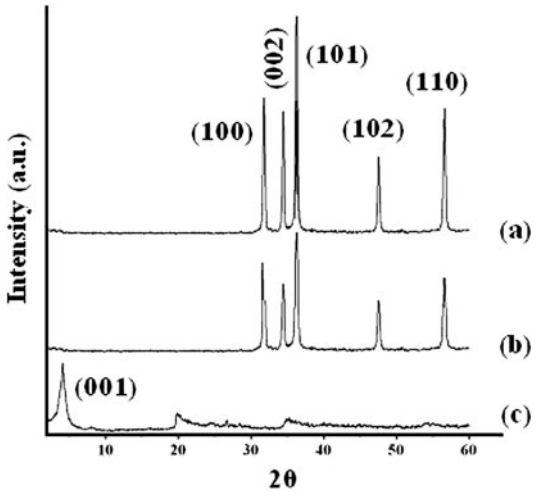

Figure 3. XRD of (a) unmodified ZnO, (b) CTAB-modified ZnO, and (c) nanoclay.

crystalline peaks for both unmodified and modified ZnO appeared above 2θ = 30° (curves a and b). The crystalline peaks appeared at 2θ = 31.9° (100), 33.3° (002), 36.4° (101), 47.7° (102), and 56.7° (110) (Leung *et al.* 2004). It was observed from curve b that position of the characteristic peaks of ZnO remained unchanged after modification. This suggested that the crystalline structure of ZnO was not influenced by the cetyl group (Hong *et al.* 2009). The organically modified nanoclay (curve c) shows a sharp peak at 2θ = 4.3°. The gallery distance calculated by using Bragg's equation was found to be 2.05 nm.

The XRD pattern of (a) untreated wood and (b) MFFA/DMDHEU/nanoclay/ZnO (1 phr)-treated, (c) MFFA/DMDHEU/nanoclay/ZnO (2 phr)-treated, (d) MFFA/DMDHEU/nanoclay/ZnO (3 phr)-treated, and (e) MFFA/DMDHEU/nanoclay/ZnO (3 phr)/plant polymer–treated wood samples is shown in Figure 4. A wide diffraction peak at 22.98° due to the (002) crystal plane of cellulose was appeared for the untreated wood (curve a) (Lü *et al.* 2006, Devi and Maji 2011). Additional small peaks appearing at 37.68° and 15.02° might be ascribed to the 040 and 101 crystal plane of cellulose I, respectively. The diffraction peak for the 040 crystal plane was much weaker than the peak for 002 crystal plane as the molecular plane of glucose found in cellulose was parallel to the 002 crystal plane (Lü *et al.* 2006). Curves b–d represent the X-ray diffractogram of WPNC treated with different percentages of ZnO (1–3 phr) and plant polymer. It was observed that the intensity of the crystalline peak of wood appearing at 2θ = 22.98° decreased in the wood composites and the first diffraction peak of nanoclay for 2θ = 4.3° disappeared. This suggested that either it was not possible to detect it by XRD or the nanoclay layers

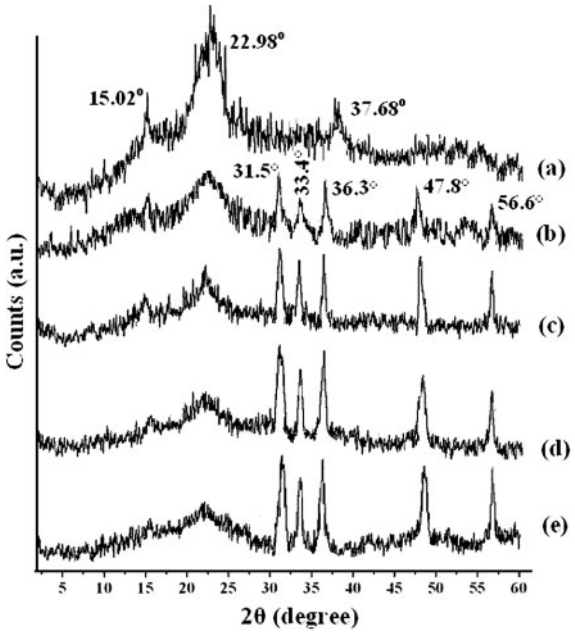

Figure 4. XRD of (a) untreated wood and (b) MFFA/DMDHEU/nanoclay/ZnO (1 phr)-treated, (c) MFFA/DMDHEU/nanoclay/ZnO (2 phr)-treated, (d) MFFA/DMDHEU/nanoclay/ZnO (3 phr)-treated, and (e) MFFA/DMDHEU/nanoclay/ZnO (3 phr)/plant polymer-treated wood samples.

became delaminated and no crystal diffraction peak appeared (Devi and Maji 2011). The peak corresponding to 37.68° disappeared and the peak appearing at 15.02° became dull. Thus, the crystallinity of wood cellulose decreases in the case of composites as some nanoparticles are inserted into the amorphous region of cellulose of wood cell walls (Lü *et al.* 2006). The characteristics peaks of ZnO appeared in diffractogram of WPNC loaded with ZnO. Higher the percentage of ZnO in the composites, higher was the intensity of the characteristics peaks of ZnO. This indicated the distribution of ZnO nanoparticles in the amorphous region of the WPNC. Similar increase in the intensity of ZnO was reported by Deka and Maji (2012) while studying the XRD pattern of WPCs treated with ZnO. The addition of plant polymer did not change significantly the diffractogram of WPNC. Thus, it could be concluded that the nanoclay layers were delaminated and the ZnO nanoparticles were incorporated in the wood.

Crystallinity determination from FTIR and XRD

Related results are shown in Table II. Although different functions were used to analyze the diffraction peaks, fitting with the Voigst functions resulted in the best fit (Wada *et al.* 1997). The recorded diffractograms were deconvoluted using Voigst function.

FTIR study was employed to find out the CrI. Figure 4 shows no lattice transformation of cellulose I to cellulose II as the peaks appearing at 15.02° and at 22.98° representing 101 and 002 plane of cellulose I were not replaced by 2θ = 12° and 21° due to prevention of transformation caused by lignin (Ishikura *et al.* 2010). A reduction in CrI values was observed for the treated wood samples. The cellulose of untreated wood showed the highest CrI while the lowest value was shown by the wood samples treated with MFFA/DMDHEU/nanoclay/ZnO (3 phr)/plant polymer. The intermolecular and intramolecular H-bonds were broken down by the MFFA, DMDHEU, nanoclay, ZnO, and plant polymer. They formed new bonds with cellulose through their hydroxyl groups, thereby lowering the rigidity of cellulose. A major fraction of cellulose remained as crystallites with interspersed amorphous region of lower extent (Marcovich *et al.* 2001). The structures of the crystallites were distorted when chemical grafting reaction took place. It was difficult for the polymers to disseminate into the crystalline region of cellulose and thus the chemical reaction occurred in the amorphous region as described by Shiraishi *et al.* (1979). The opening of some hydrogen-bonded cellulose chains occurred by reacting the polymers at the chain end on the surface of the crystallites. Thus, some new amorphous cellulose was produced and it continued with the progress of reaction (Marcovich *et al.* 2001). CrI determined from XRD analysis was also shown in Table II. The results were in good agreement with the values obtained from FTIR studies. This indicated a clear reduction in crystallinity of cellulose due to treatment with DMDHEU, nanoclay, ZnO, and plant polymer.

Morphological studies of the nanocomposites

The EDX of the plant polymer and the composite are represented in Figure 5. It was observed from the spectrum (Figure 5a) that the plant polymer contained C, O, P, and Ca. The occurrence of phosphorus in the plant polymer contributed to its FR behavior. Ghosh *et al.* (2001) found similar results while studying the EDX analysis of plant polymer. The spectrum of wood treated with MFFA/DMDHEU/nanoclay/ZnO (3 phr)/plant polymer is shown in Figure 5b. The composite contained C, O, N, Na, Mg, Al, Si, Zn, and P. It was evident from the spectrum that all the components were successfully impregnated into the wood. The presence of nitrogen from MFFA and DMDHEU and phosphorus from the plant polymer significantly contributed the FR characteristics of the composites. The SEM micrographs of untreated and treated wood samples are shown in Figure 6. The vacant cell wall, pits, and parenchymas seen in untreated wood (Figure 6a) were filled up by MFFA/DMDHEU (Figure 6b). The nanoclay and ZnO were traced as some white spots located either in cell lumen or cell wall (Figure 6c–f). Figure 7 shows the TEM micrographs of untreated and treated wood samples. There was no observation of the orientation of cell wall components in untreated wood (Figure 7a). The nanoclay and ZnO nanoparticles, which were dispersed in the cell wall or lumen along with polymer matrix, could be seen as black slices and black spots, respectively (Figure 7b–e).

UV resistance study

Figure 8 represents the weight loss of untreated and treated wood samples exposed to an UV environment for different time periods. Due to the

Table II. CrI values of cellulose matrix of untreated and treated wood samples calculated by the area method before and after UV exposure.

Samples		Untreated wood	MFFA/DMDHEU treated	MFFA/DMDHEU/Nanoclay/ZnO (1 phr) treated	MFFA/DMDHEU/Nanoclay/ZnO (2 phr) treated	MFFA/DMDHEU/Nanoclay/ZnO (3 phr) treated	MFFA/DMDHEU/Nanoclay/ZnO (3 phr)/plant polymer treated
XRD results	Before irradiation	63.21	53.12	41.23	37.67	34.43	33.51
FTIR results	After irradiation	62.53	54.22	40.56	37.81	35.62	32.65
FTIR results	10 days	60.34	52.33	39.37	36.58	34.69	31.45
	20 days	57.21	49.87	36.54	35.62	33.72	28.78
	30 days	52.76	46.58	35.78	34.39	31.46	27.85
	40 days	49.88	45.32	34.28	32.47	30.57	26.98
	50 days	47.54	43.27	32.56	31.42	29.76	26.03
	60 days	46.53	42.16	31.64	30.12	28.43	25.63

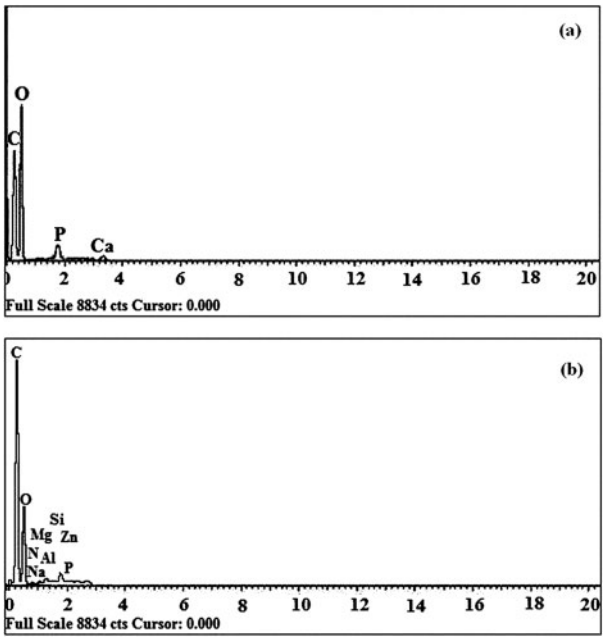

Figure 5. EDX of (a) plant polymer and (b) wood treated with MFFA/DMDHEU/nanoclay/ZnO (3 phr)/plant polymer.

moisture uptake at the early stage of exposure time, a small increase in weight was found for all the samples. This early increase in weight was higher than the material loss induced by the degradation. The maximum weight loss (%) was seen in the untreated wood samples followed by the treated ones after 60 days of irradiation. With an increase in the amount of ZnO, the rate of weight loss decreased. ZnO possesses a wide band gap that is transparent in the visible range and absorbs the UV rays upon exposure to UV irradiation. Minimum weight loss was shown by the samples when plant polymer was added to the system.

Figure 9 shows the change of carbonyl index values with time for untreated and treated wood samples. The increase of carbonyl index values was due to chain scission of the polymer and wood. The chain scission decreased the density of entanglement of the polymer chains and hence a decrease in weight was observed. Untreated wood (curve 9a) has the highest carbonyl index values due to higher oxidation of wood cellulose. The samples treated with MFFA/DMDHEU/nanoclay/ZnO (3 phr)/plant polymer showed the lower carbonyl index value (curve 9f). The incorporation of MFFA/DMDHEU decreased the carbonyl index value. The cross-linking provided by DMDHEU might be responsible for delayed photodegradation of the composites. The value decreased further when nanoclay and ZnO were added along with MFFA/DMDHEU to the wood (curves 9c–e). The higher the amount of ZnO, the lower the carbonyl index value. Both nanoclay and ZnO stabilized the composite by providing a barrier to UV radiation and hence delayed the

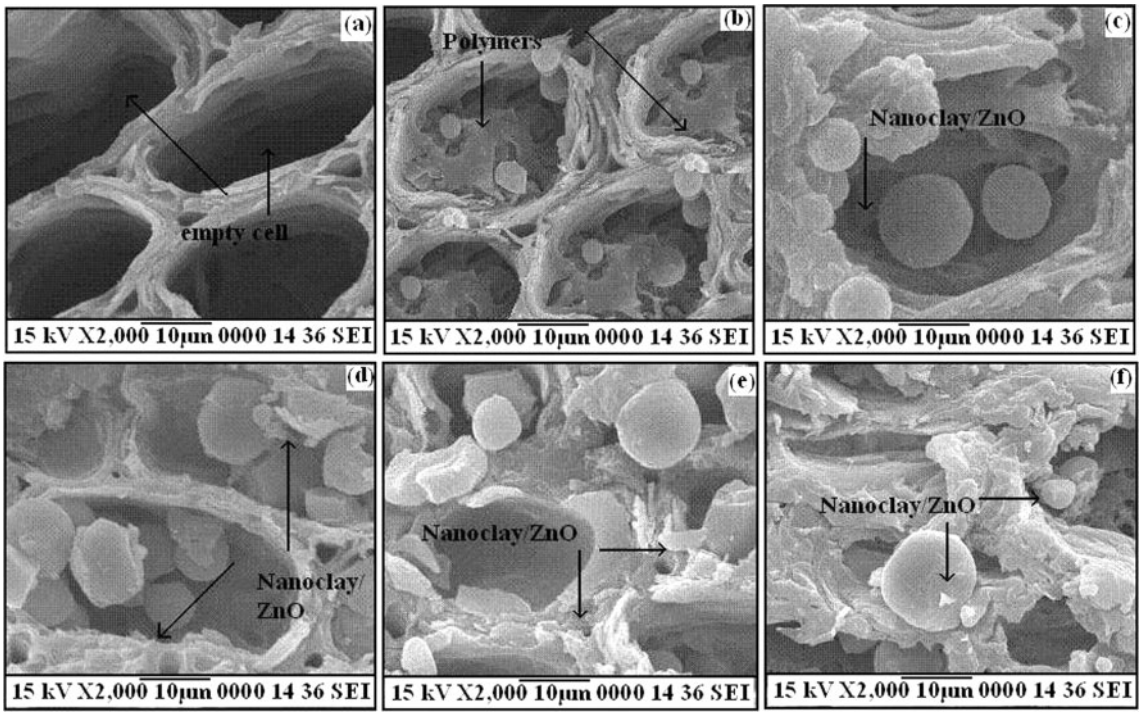

Figure 6. SEM micrographs of wood (a) untreated and treated with (b) MFFA/DMDHEU, (c) MFFA/DMDHEU/nanoclay/ZnO (1 phr), (d) MFFA/DMDHEU/nanoclay/ZnO (2 phr), (e) MFFA/DMDHEU/nanoclay/ZnO (3 phr), and (f) MFFA/DMDHEU/nanoclay/ZnO (3 phr)/plant polymer.

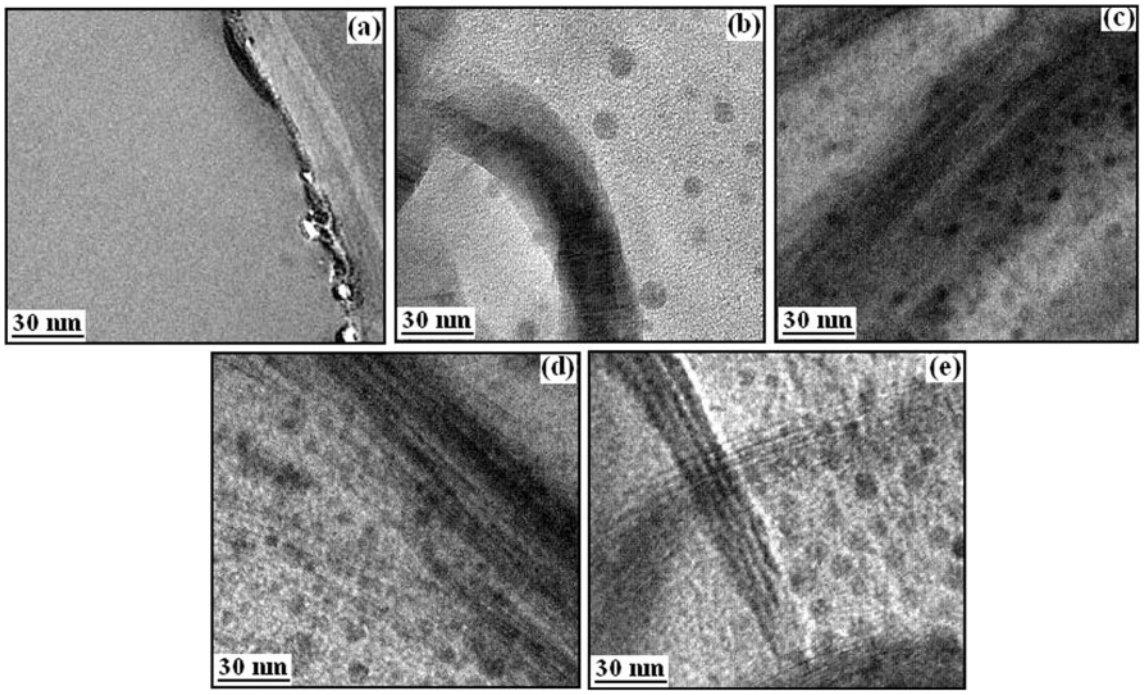

Figure 7. TEM micrographs of (a) untreated and (b) MFFA/DMDHEU/nanoclay/ZnO (1 phr)-treated, (c) MFFA/DMDHEU/nanoclay/ZnO (2 phr)-treated, (d) MFFA/DMDHEU/nanoclay/ZnO (3 phr)-treated, and (e) MFFA/DMDHEU/nanoclay/ZnO (3 phr)/plant polymer–treated wood samples.

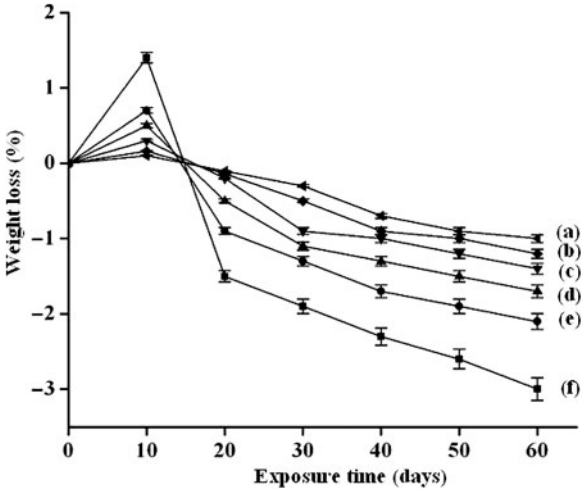

Figure 8. Weight losses versus exposure time of (a) untreated wood and wood treated with (b) MFFA/DMDHEU, (c) MFFA/DMDHEU/nanoclay/ZnO (1 phr), (d) MFFA/DMDHEU/nanoclay/ZnO (2 phr), (e) MFFA/DMDHEU/nanoclay/ZnO (3 phr), and (f) MFFA/DMDHEU/nanoclay/ZnO (3 phr)/plant polymer.

photodegradation process, as well as improved the UV resistance. Similar UV stability of PP nanocomposite was reported by Zhao and Li (2006) after the incorporation of ZnO. Grigoriadou *et al.* (2011) reported an increase in UV stability on addition of montmorillonite clay in high-density polyethylene (HDPE). The plant polymer enhanced the interaction among wood, MFFA, clay, and ZnO through its hydroxyl groups resulting in a decrease of the photodegradation process. This in turn showed the lower carbonyl index value.

Figure 10 shows the LI values with time for untreated and treated wood samples. LI value decreased with an increase in the UV exposure time. The trend of the LI value followed the order: MFFA/DMDHEU/nanoclay/ZnO (3 phr)/plant polymer-treated > MFFA/DMDHEU/nanoclay/ZnO (3 phr)-treated > MFFA/DMDHEU/nanoclay/ZnO (2 phr)-treated > MFFA/DMDHEU/nanoclay/ZnO (1 phr)-treated > MFFA/DMDHEU-treated > untreated wood samples. ZnO protected the lignin decay of wood from the UV radiation by preventing the formation of quinones, carbonyls, or peroxides. Patachia *et al.* (2012) reported that LI values of ionic liquid–treated wood decrease on exposure to UV.

Figure 11 shows the FTIR spectra of the untreated and treated wood samples upon exposure to UV rays for 60 days. Untreated wood had the highest carbonyl peak intensity and the treated wood samples had lower peak intensity. It was also observed that after irradiation, the characteristic peak for lignin almost disappeared in the case of untreated wood and treatment of the samples with polymer, nanoclay, and ZnO enhanced the lignin stability. Hence, the decrease of lignin peak intensity was less pronounced in case of treated wood samples.

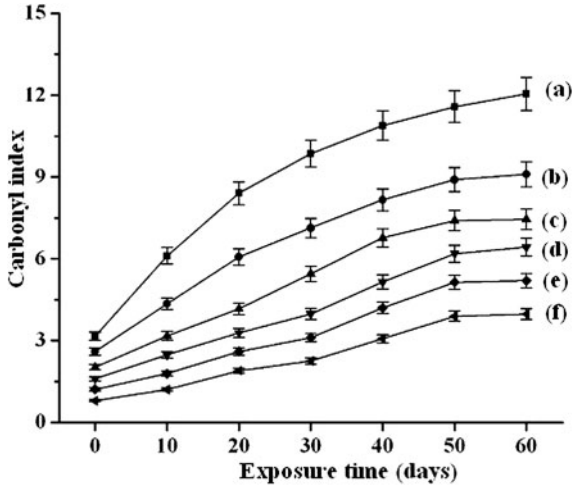

Figure 9. Carbonyl index values of (a) untreated wood and wood treated with (b) MFFA/DMDHEU, (c) MFFA/DMDHEU/nanoclay/ZnO (1 phr), (d) MFFA/DMDHEU/nanoclay/ZnO (2 phr), (e) MFFA/DMDHEU/nanoclay/ZnO (3 phr), and (f) MFFA/DMDHEU/nanoclay/ZnO (3 phr)/plant polymer.

Table II shows the variation of CrI values of the untreated and treated wood samples on exposure to UV rays for different time period. The CrI values were calculated from FTIR spectra (not shown). Untreated wood showed higher CrI compared to treated wood samples. In both untreated and treated wood samples, CrI was found to decrease with an increase in exposure time to UV light. Furthermore, the rate of decrease of CrI was more in untreated wood than treated wood. DMDHEU, nanoclay, and plant polymer enhanced the interfacial interaction, while ZnO provided the protective barrier against UV light. Thus, the treated wood samples would undergo less degradation and hence exhibit a lower rate of decrease in CrI. A similar decrease in crystalinity index values was observed by Patachia *et al.* (2012) while studying the UV degradation of ionic liquid–treated wood.

SEM micrographs of samples after 60 days of exposure are shown in Figure 12. Cracks appeared and degradation occurred on the surface of untreated wood (Figure 12a). The surface of wood treated with MFFA/DMDHEU (Figure 12b) was more uneven compared to samples treated with MFFA/DMDHEU/nanoclay/ZnO (Figure 12c). With the increase in the percentage of ZnO, the surface smoothness of the composites was found to increase. This indicated the shielding effect of ZnO nanoparticles to UV rays. Addition of plant polymer to the ZnO-treated samples retarded further the formation of cracks on surface of the samples. The plant polymer facilitated the interfacial interaction between wood, ZnO, nanoclay, and MFFA polymer and hence protected the composite from degradation against UV rays.

The mechanical properties of the samples are shown in Table III after 60 days of irradiation. It was observed that highest loss of mechanical properties was observed in case of untreated wood. However, loss was less significant when ZnO and nanoclay were added to the MFFA/DMDHEU-treated wood samples. With an increase in the amount of ZnO, further reduction in loss of tensile and flexural values was noticed. ZnO shielded the composites, thus offering resistance to UV rays.

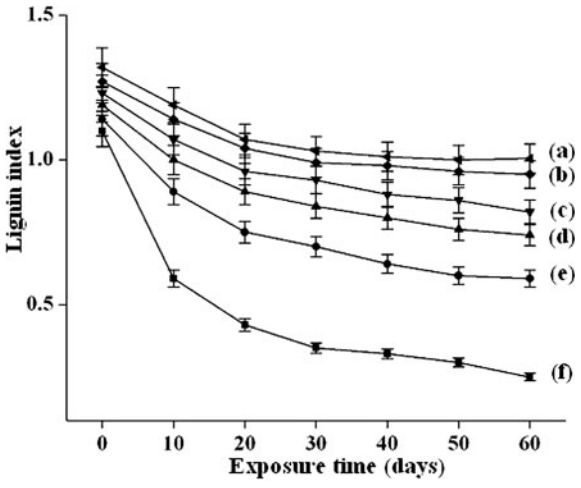

Figure 10. LI values of wood treated with (a) MFFA/DMDHEU/nanoclay/ZnO (3 phr)/plant polymer, (b) MFFA/DMDHEU/nanoclay/ZnO (3 phr), (c) MFFA/DMDHEU/nanoclay/ZnO (2 phr), (d) MFFA/DMDHEU/nanoclay/ZnO (1 phr), (e) MFFA/DMDHEU, and (f) untreated wood samples.

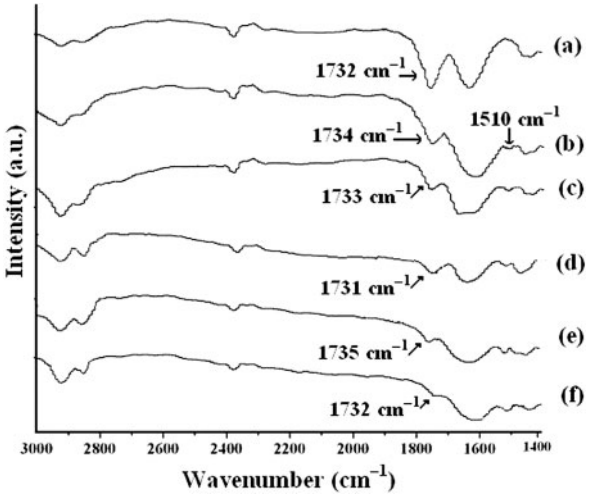

Figure 11. Change in carbonyl and lignin peak intensity of (a) untreated wood and wood treated with (b) MFFA/DMDHEU, (c) MFFA/DMDHEU/nanoclay/ZnO (1 phr), (d) MFFA/DMDHEU/nanoclay/ZnO (2 phr), (e) MFFA/DMDHEU/nanoclay/ZnO (3 phr), and (f) MFFA/DMDHEU/nanoclay/ZnO (3 phr)/plant polymer.

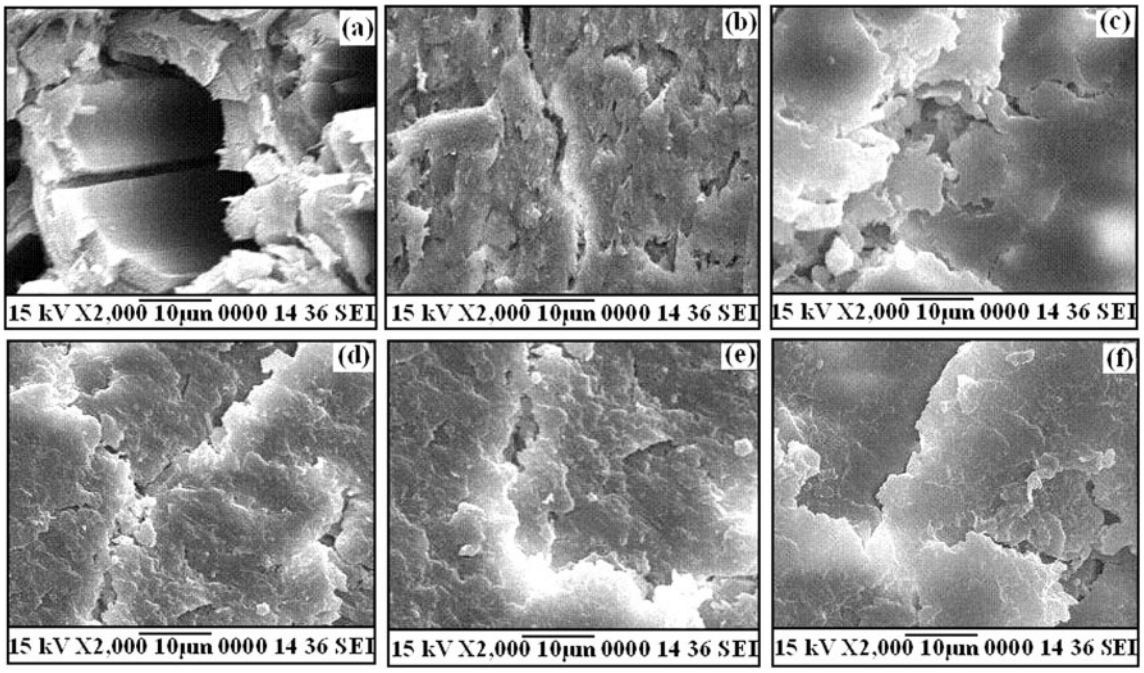

Figure 12. SEM micrographs of UV-treated samples after 60 days. (a) Untreated wood and wood treated with (b) MFFA/DMDHEU, (c) MFFA/DMDHEU/nanoclay/ZnO (1 phr), (d) MFFA/DMDHEU/nanoclay/ZnO (2 phr), (e) MFFA/DMDHEU/nanoclay/ZnO (3 phr), and (f) MFFA/DMDHEU/nanoclay/ZnO (3 phr)/plant polymer.

Mechanical properties

Table III shows the tensile and flexural values of untreated and treated wood samples. It was observed that the treatment of the samples with MFFA/DMDHEU would lead to an increase in tensile and flexural values. DMDHEU enhanced the interfacial interaction between wood and MFFA, resulting in increased values (Xie *et al.* 2010). A perceptible improvement in tensile and flexural values was observed upon inclusion of nanoclay and ZnO to the WPC samples. At a fixed clay loading (3 phr), the higher the amount of ZnO, the higher was the tensile and flexural values. The silicate layers would bind the polymer chains in their gallery layers, thereby stiffening the composites. The cetyl group and surface hydroxyl group present in CTAB-modified ZnO enhanced its interaction between wood, MFFA, DMDHEU, and clay (Deka and Maji 2012). Samples treated with MFFA/plant polymer/DMDHEU/nanoclay/ZnO/plant polymer had the highest improvement in properties. The abundant hydroxyl groups present in plant polymer facilitated the interaction between wood, MFFA, DMDHEU, clay, and ZnO.

Limiting oxygen index

The LOI values of treated and untreated wood are shown in Table IV. Treated wood samples showed higher LOI values than the untreated ones. Higher LOI value of MFFA/DMDHEU-treated samples was due to the synergistic effect of MFFA and DMDHEU (Wu and Yang 2004). Both contains nitrogen and on combustion oxides of nitrogen were produced which displaced the oxygen present on the surface of the composites. Nanoclay promoted char formation. The char produced an insulated layer over the samples and thus increased its flame resistance property (Gilman *et al.* 2000). With an increase in the amount of modified ZnO, the flame retardancy would increase as it could protect the samples from heat and oxygen. Addition of plant polymer would amplify the flame retardancy of the composites to a considerable amount because of its phosphorus content (Ghosh and Maiti 1998; Jana *et al.* 2000).

Thermal stability

Table IV shows the initial decomposition temperature (T_i), maximum pyrolysis temperature (T_m), and residual weight (%) (RW) for untreated and polymer-treated wood samples. Noncombustible material, moisture, and CO_2 are produced in the temperature range between 100 and 200°C. T_i values improved after treatment of the samples with MFFA/DMDHEU. The incorporation of nanoclay and ZnO in the samples further enhanced the T_i values. Maximum T_i value was observed for MFFA/DMDHEU/nanoclay/ZnO (3 phr)/plant polymer (3 phr)–treated wood samples.

Table III. Flexural and tensile properties of untreated and treated wood before and after UV degradation.

	Flexural properties				Tensile properties			
	Before degradation		After degradation		Before degradation		After degradation	
Sample	Strength (MPa) (±SD)	Modulus (MPa) (±SD)	Strength (MPa) (±SD)	Modulus (MPa) (±SD)	Strength (MPa) (±SD)	Modulus (MPa) (±SD)	Strength (MPa) (±SD)	Modulus (MPa) (±SD)
Untreated wood	118.07 (±0.58)	5922.54 (±0.45)	100.89 (±0.66)	5018.64 (±0.87)	41.15 (±0.76)	305.23 (±10.13)	30.11 (±0.43)	223.34 (±9.76)
MFFA/DMDHEU	127.64 (±0.86)	6402.58 (1.12)	119.76 (±0.53)	6009.55 (±1.01)	48.75 (±1.01)	361.62 (±9.57)	39.23 (±0.38)	290.98 (±7.87)
MFFA/DMDHEU/nanoclay/ZnO (1 phr)	139.13 (±0.75)	6978.93 (±0.68)	132.33 (±0.47)	6639.81 (±0.26)	64.91 (±1.08)	481.46 (±12.46)	58.75 (±0.56)	435.77 (±8.43)
MFFA/DMDHEU/nanoclay/ZnO (2 phr)	140.35 (±1.05)	7040.13 (±1.03)	135.58 (±0.28)	6803.40 (±0.92)	65.53 (±0.75)	486.06 (±16.78)	61.13 (±0.64)	453.43 (±8.98)
MFFA/DMDHEU/nanoclay/ZnO (3 phr)	142.68 (±0.64)	7157.03 (±0.76)	139.86 (±0.51)	7018.17 (±0.54)	67.83 (±1.22)	503.12 (±8.63)	64.86 (±0.82)	481.09 (±10.21)
MFFA/DMDHEU/nanoclay/ZnO (3 phr)/plant polymer (3 phr)	143.57 (±0.87)	7207.16 (±1.23)	140.63 (±0.36)	7056.81 (±1.12)	68.46 (±1.87)	507.80 (±7.84)	66.26 (±1.45)	491.48 (±11.13)

SD, standard deviation.

Table IV. Thermal degradation of untreated and treated wood samples.

				Temperature of decomposition (T_D) in °C at different weight loss (%)					
Sample	T_i	T_m [a]	T_m [b]	20%	40%	60%	80%	RW% at 600 °C	LOI (%) (±SD)
Untreated wood	161	302	395	267	294	332		27.82	21(±0.33)
Wood treated with									
MFFA/DMDHEU	238	338	431	304	330	360	424	8.2	26 (±0.25)
MFFA/DMDHEU/nanoclay/ZnO (1 phr)	268	366	455	341	357	390	459	20.41	37 (±0.67)
MFFA/DMDHEU/nanoclay/ZnO (2 phr)	271	369	458	343	359	394	461	21.23	38 (±0.43)
MFFA/DMDHEU/nanoclay/ZnO (3 phr)	274	372	461	346	361	396	463	22.02	40 (±0.41)
MFFA/DMDHEU/nanoclay/ZnO (3 phr)/plant polymer	276	375	463	348	364	398	466	22.04	42 (±0.72)

SD, standard deviation.

T_m values were also higher for the treated wood than untreated ones. T_m values for the first stage of pyrolysis was due to the depolymerization of hemicellulose, glycosidic linkage of cellulose, thermal decomposition of cellulose, and disintegration of interunit linkages and condensation of aromatic rings during pyrolytic degradation of lignin (Marcovich *et al.* 2001). The second stage of pyrolysis was due to the degradation of polymers. Improvement of thermal stability of wood treated with MFFA/DMDHEU was associated with the formation of cross-linked structure with cell wall of wood. The combined effect of nanoclay and ZnO had a significant effect on enhancing the thermal stability of the composites. The silicate layers of nanoclay provided a meandering path, thus delaying the diffusion of volatile product through the prepared composites (Qin *et al.* 2004). ZnO interacted with the wood, nanoclay, and polymer through its surface hydroxyl groups and cetyl groups. Laachachi *et al.* (2009) found an improvement in thermal stability of poly-methylmethacrylate (PMMA) composite after addition of organo-montmorillonite (MMT) and ZnO into PMMA. Incorporation of plant polymer would further improve the thermal stability of the composites due to the presence of phosphorus (4.34%, w/w) (Ghosh and Maiti 1998).

RW (%) value of untreated wood was highest while the value for treated wood with MFFA/DMDHEU was lowest. The volatile components diffused out and the lignin present in the wood contributed to char formation. The addition of nanoclay and ZnO would increase the char formation and thus would further prevent the thermal degradation by forming a protective insulating layer.

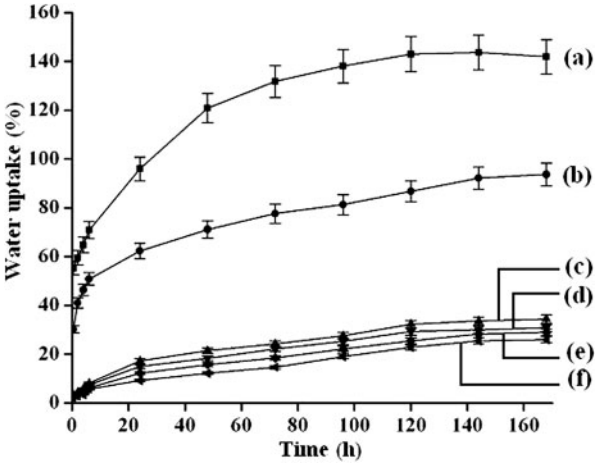

Figure 13. Water absorption test of wood (a) untreated and treated with (b) MFFA/DMDHEU, (c) MFFA/DMDHEU/nanoclay/ZnO (1 phr), (d) MFFA/DMDHEU/nanoclay/ZnO (2 phr), (e) MFFA/DMDHEU/nanoclay/ZnO (3 phr), and (f) MFFA/DMDHEU/nanoclay/ZnO (3 phr)/plant polymer.

Water uptake test

The water uptake capacity of untreated and treated wood samples is shown in Figure 13. Untreated wood showed the highest water absorption capacity. Wood consists of native cellulose, which had a rigid structure and the rest of the components present in wood are amorphous substances accessible to water molecules. MFFA/DMDHEU was impregnated into the cell wall of wood and impeded the water penetration by a bulk effect. DMDHEU could form cross-link with the cell wall and prevented water incursion into the composite (Xie *et al.* 2010). MFFA/DMDHEU/nanoclay/ZnO treatment offered higher water repellence, and with an increase in the amount of ZnO, the water repellency would increase. ZnO in combination with nanoclay would occupy the void spaces in wood and would make the cell wall more bulky. The plant polymer contains plenty of available hydroxyl groups, which enhanced interaction with wood, MFFA, DMDHEU, nanoclay, and ZnO, and thus improved the water resistance.

Conclusion

WPCs are extensively used in structural components including window/window profiles, decking, railing, table tops, partition walls, trim parts in dashboards, door panels, parcel shelves, and cabin linings. It is a low-cost, easily available, and high-end value product. The worldwide manufacture of WPCs will increase from 2.43 million tons in 2012 to 3.83 million tons in 2015 as reported by market research. The replacement of pure wood by the WPCs in the various construction applications leads to an increased service life of the material; moreover, its maintenance cost is also reduced as it is resistant to rot and decay and has much more improved properties than the untreated wood. The treated wood also has less environmental impact as it does not eliminate any toxic volatile organic compounds that are harmful to human health as well as environment. Impregnation of wood with ZnO, nanoclay, and plant polymer along with MFFA/DMDHEU under vacuum condition could influence the water uptake capacity and the mechanical, thermal, flame-retardant, and UV-resistant properties. The surface modification of ZnO by CTAB was confirmed by FTIR. XRD and FTIR studies indicated the formation of the composites, and a decrease in crystallinity of cellulose was observed from 63.2 to 33.5 as determined from CrI. The morphology of the nanocomposites was studied by SEM. A uniform distribution of the nanoparticles was observed from TEM analysis. WPNC loaded with nanoclay, ZnO, and plant polymer showed an improvement in properties like

mechanical, thermal, and flame-retardant properties. The incorporation of plant polymer has a remarkable effect on the thermal and FR properties of the composites. The water uptake capacity was found to reduce from 141.5% to 25.8%. The UV resistance of the composites was increased significantly after incorporation of ZnO and plant polymer into the composites as was evidenced by weight loss, carbonyl index, LI, CrI values, SEM, and lower mechanical properties loss. The ZnO nanoparticles can effectively act as a screen for the composites thus enhancing its UV resistance properties. Maximum properties improvement was found in WPCs loaded with 3 phr each of nanoclay, ZnO, and plant polymers. Thus, this softwood that merely remains unused as biowaste and is mainly used in fuel applications can be made a value-added material suitable for various structural applications through the formation of WPCs.

References

Bajia, S., Sharma, R. and Bajia, B. (2009) Solid-state microwave synthesis of melamine-formaldehyde resin. *E Journal of Chemistry*, 6(1), 120–124.

Bhattacharya, S. B., Das, A. K. and Banerji, N. (1982) Chemical investigations on the gum exudate from sajna (*Moringa oleifera*). *Carbohydrate Research*, 102(1), 253–262.

Cai, X., Riedl, B., Zhang, S. Y. and Wan, H. (2008) The impact of the nature of nanofillers on the performance of wood polymer nanocomposites. *Composites Part A: Applied Science and Manufacturing*, 39(5), 727–737.

Deka, B. K. and Maji, T. K. (2010) Effect of coupling agent and nanoclay on properties of HDPE, LDPE, PP, PVC blend and *Phargmites karka* nanocomposite. *Composites Science and Technology*, 70(12), 1755–1761.

Deka, B. K. and Maji, T. K. (2012) Effect of nanoclay and ZnO on the physical and chemical properties of wood polymer nanocomposite. *Journal of Applied Polymer Science*, 124(4), 2919–2929.

Devi, R. R. and Maji, T. K. (2011) Preparation and characterization of wood/styrene-acrylonitrile copolymer/MMT nanocomposite. *Journal of Applied Polymer Science*, 122(3), 2099–2109.

Devi, R. R. and Maji, T. K. (2012) Effect of nano-ZnO on thermal, mechanical, UV stability, and other physical properties of wood polymer composites. *Industrial and Engineering Chemistry Research*, 51(10), 3870–3880.

Devi, R. R., Saikia, C. N., Thakur, A. J. and Maji, T. K. (2007) Modification of rubber wood with styrene in combination with diethyl allyl phosphate as the flame-retardant agent. *Journal of Applied Polymer Science*, 105(5), 2461–2467.

Dhoke, S. K., Khanna, A. S. and Sinha, T. J. M. (2009) Effect of nano-ZnO particles on the corrosion behavior of alkyd-based waterborne coatings. *Progress in Organic Coatings*, 64(4), 371–382.

Esteves, B., Nunes, L. and Pereira, H. (2011) *Properties of furfurylated wood (Pinus pinaster) Eigenschaften von furfuryliertem Kiefernholz (Pinus pinaster)*. *European Journal of Wood and Wood Products*, 69(4), 521–525.

Ghosh, S. N., Ghosh, A. K., Adhikari, B. and Maiti, S. (2001) Characterization of a flame retardant plant polymer and its influence on the properties of rubber vulcanizate. *International Journal of Polymeric Materials*, 48(1), 79–97.

Ghosh, S. N. and Maiti, S. (1998) Adhesive performance, flammability evaluation and biodegradation study of plant polymer blends. *European Polymer Journal* 34(5–6), 849–854.

Gilman, J. W., Jackson, C. L., Morgan, A. B., Harris, R. H., Manias, E., Giannelis, E. P., Wuthenow, M., Hilton, D. and Phillips, S. H. (2000) Flammability properties of polymer-layered-silicate nanocomposites: Polypropylene and polystyrene nanocomposites. *Chemistry of Materials*, 12(7), 1866–1873.

Gindl, W., Zargar-Yaghubi, F. and Wimmer, R. (2003) Impregnation of softwood cell walls with melamine-formaldehyde resin. *Bioresource Technology*, 87(3), 325–330.

Grigoriadou, I., Paraskevopoulos, K. M., Chrissafis, K., Pavlidou, E., Stamkopoulos, T.-G. and Bikiaris, D. (2011) Effect of different nanoparticles on HDPE UV stability. *Polymer Degradation and Stability*, 96(1), 151–163.

Hazarika, A. and Maji, T. K. (2013) Effect of different cross-linkers on properties of melamine formaldehyde-furfuryl alcohol copolymer/montmorillonite impregnated softwood (*Ficus hispida*). *Polymer Engineering and Science*, 53(7), 1394–1404.

Hazarika, A. and Maji, T. K. (2014) Strain sensing behavior and dynamic mechanical properties of carbon nanotubes/nanoclay reinforced wood polymer nanocomposite. *Chemical Engineering Journal*, 247, 33–41.

Hazarika, A. and Maji, T. K. (2014) Thermal decomposition kinetics, flammability, and mechanical property study of wood polymer nanocomposite. *Journal of Thermal Analysis and Calorimetry*, 115(2), 1679–1691.

Hong, R. Y., Li, J. H., Chen, L. L., Liu, D. Q., Li, H. Z., Zheng, Y. and Ding, J. (2009) Synthesis, surface modification and photocatalytic property of ZnO nanoparticles. *Powder Technology*, 189(3), 426–432.

Ishikura, Y., Abe, K. and Yano, H. (2010) Bending properties and cell wall structure of alkali-treated wood. *Cellulose*, 17(1), 47–55.

Jana, T., Roy, B. C. and Maiti, S. (2000) Biodegradable film. *Polymer Degradation and Stability*, 69(1), 79–82.

Jang, T. R., Sheu, T. C., Sheu, J. J. and Chen, C. C. (1993) Crosslinking of cotton fabrics premercerized with different alkalis. Part III: Crosslinking and physical properties of DMDHEU-treated fabrics. *Textile Research Journal*, 63(11), 679–686.

Laachachi, A., Ruch, D., Addiego, F., Ferriol, M., Cochez, M. and Lopez Cuesta, J.-M. (2009) Effect of ZnO and organo-modified montmorillonite on thermal degradation of poly(methyl methacrylate) nanocomposites. *Polymer Degradation and Stability*, 94(4), 670–678.

Lande, S., Westin, M. and Schneider, M. (2004) Properties of furfurylated wood. *Scandinavian Journal of Forest Research*, 19(suppl 5), 22–30.

Leung, Y. H., Djurišic, A. B., Gao, J., Xie, M. H., Wei, Z. F., Xu, S. J. and Chan, W. K. (2004) Zinc oxide ribbon and comb structures: synthesis and optical properties. *Chemical Physics Letters*, 394(4-6), 452–457.

Li, H. and Tripp, C. P. (2002) Spectroscopic identification and dynamics of adsorbed cetyltrimethylammonium bromide structures on TiO_2 surfaces. *Langmuir*, 18(24), 9441–9446.

Lori, J. A., Myina, O. M., Ekanem, E. J. and Lawal, A. O. (2011) Structural and adsorption characteristics of carbon adsorbent synthesized from polyfurfuryl alcohol with kaolinite template. *Research Journal of Applied Sciences, Engineering and Technology*, 3, 440–446.

Lü, W. H., Zhao, G. J. and Xue, Z. H. (2006) Preparation and characterization of wood/montmorillonite nanocomposites. *Forestry Studies in China*, 8(1), 35–40.

Marcovich, N. E., Reboredo, M. M. and Aranguren, M. I. (2001) Modified woodflour as thermoset fillers. *Thermochimica Acta*, 372(1-2), 45–57.

Patachia, S., Croitoru, C. and Friedrich, C. (2012) Effect of UV exposure on the surface chemistry of wood veneers treated with ionic liquids. *Applied Surface Science*, 258(18), 6723–6729.

Qin, H., Zhang, S., Zhao, C., Feng, M., Yang, M. Shu, Z., & Yang, S. 2004. Thermal stability and flammability of polypropylene/montmorillonite composites. *Polymer Degradation and Stability*, 85(2), 807–813.

Schneider, M. H. H. (1995) New cell wall and cell lumen wood polymer composites. *Wood Science and Technology*, 29(2), 135–158.

Shiraishi, N., Matsunaga, T., Yokota, T. and Hayashi, Y. (1979) Preparation of higher aliphatic acid esters of wood in an N_2O_4–DMF cellulose solvent medium. *Journal of Applied Polymer Science*, 24 (12), 2347–2359.

Stark, N. M. and Matuana, L. M. (2004) Surface chemistry changes of weathered HDPE/wood-flour composites studied by XPS and FTIR spectroscopy. *Polymer Degradation and Stability*, 86(1), 1–9.

Venas, T. M. and Rinnan A. (2008) Determination of weight percent gain in solid wood modified with in situ cured furfuryl alcohol by near-infrared reflectance spectroscopy. *Chemometrics and Intelligent Laboratory Systems*, 92, 125–130.

Wada, M., Okano, T. and Sugiyama, J. (1997) Synchrotron-radiated X-ray and neutron diffraction study of native cellulose. *Cellulose*, 4(3), 221–232.

Wu, W. and Yang, C. Q. (2004) Statistical analysis of the performance of the flame retardant finishing system consisting of a hydroxy-functional organophosphorus oligomer and the mixture of DMDHEU and melamine–formaldehyde resin. *Polymer Degradation and Stability*, 85(1), 623–632.

Xie, Y., Xiao, Z., Grüneberg, T., Militz, H., Hill, C. A. S., Steuernagel, L. and Mai, C. (2010) Effects of chemical modification of wood particles with glutaraldehyde and 1,3-dimethylol-4,5-dihydroxyethyleneurea on properties of the resulting polypropylene composites. *Composites Science and Technology*, 70(13), 2003–2011.

Zhao, H. and Li, R. K. Y. (2006) A study on the photodegradation of zinc oxide (ZnO) filled polypropylene nanocomposites. *Polymer*, 47(9), 3207–3217.